

Short-Period APPLE II Undulator for Generating 12-15 keV X-Rays at the Advanced Photon Source

(formerly MD-TN-2008-001)

R. Dejus – MD Group/ASD
S. Sasaki – Hiroshima Synchrotron Radiation Center,
Higashi-Hiroshima, 739-0046, Japan

Rev. 3, November 25, 2009: Edited by C. Eyberger for release as cleared document
ANL/APS/LS-313; updated in ICMS.

Rev. 2, December 11, 2008: Entry into the ICMS

Rev. 1, March 26, 2008: Minor edits

Rev. 0, March 24, 2008: Initial release as Technical Note MD-TN-2008-001

Introduction

A request was made by a user group at the Advanced Photon Source to provide a design of an undulator generating intense hard x-rays over a limited photon energy range (12 – 15 keV), with very small x-ray “contamination” at higher energies. For their scientific program (and technique used), the x-ray images obtained are sensitive to inherent imperfections in the beamline optical components, hence traditional components, such as mirrors and monochromators to modify the spectral content of the x-ray beam, cannot be used. Therefore, the x-ray spectrum needs to be tailored directly at the source to satisfy their needs. A pure “single-line” x-ray undulator source does not exist. However, we may construct an undulator that optimizes the flux in the requested energy range while limiting the flux at higher energies.

Such an undulator would need to fulfill the following two criteria:

- It operates at a small K value (< 1.0), and
- It generates circularly polarized light.

Because there are no requirements regarding polarization, i.e., either circular or planar polarization may be used, a circularly polarizing undulator is being proposed because the higher-order harmonics will be greatly suppressed (for a zero-emittance electron beam, all radiation on-axis above the first harmonic will be zero). However, for a finite-size aperture and finite beam emittance, the suppression will be less than ideal. But the suppression is large enough to warrant the extra effort involved using a more complicated design. The proposed undulator is constructed of pure permanent magnets. Because the polarization would be fixed, there is no need to translate the jaws longitudinally; hence it is a simplified design compared to the traditional APPLE II design.

In this note, we present magnet design calculations and radiation calculations for an optimized helical undulator and compare its performance to i) Undulator A, and ii) a planar undulator with the same period length as the helical device. The proposed helical undulator is

optimized for high brilliance and high photon flux in the energy range 12 – 15 keV. For example, it produces over four times more power in the central cone of the first harmonic than Undulator A at 12.9 keV, while maintaining similar higher harmonic content! Because of the small K value, there are no issues regarding power management even in the future for high-current storage ring operations at 200 mA. The code XOP¹ was used to calculate the flux spectra from ideal undulators with no magnetic field errors, and the code TCAP² was used to calculate the on-axis aperture flux tuning curves (field errors are not important for the first harmonic and for the issues discussed in this note).

Magnet Modeling of APPLE II Design

Preliminary magnetic design calculations were performed using the code RADIA³ to minimize the period length at a 11.0-mm gap. The shorter the period length, the higher the on-axis brilliance and flux for a given harmonic energy. It was found that a period length of 2.6 cm would be feasible to use and yet reach a minimum first-harmonic energy of about 12 keV. A schematic of the APPLE II undulator (not full length) is shown in Fig. 1. The APPLE II undulator consists of pure permanent magnets in four independent movable jaws (two jaws are located above the electron beam orbit and two jaws below).⁴ However, because there is no need to change the polarization for this particular device, the jaws will be fixed longitudinally.

The permanent magnet material is NdFeB, grade N39UH from Shin-Etsu, with a vendor-specified minimum B_r of 1.22 Tesla. Each magnet block has the dimensions 3.0 (X) x 3.0 (Y) x $\lambda/4$ (Z) cm³, where λ is the period length (see Fig. 1). These dimensions were set so that the device would fit into the existing insertion device vacuum chamber at the APS using the standard support structure.

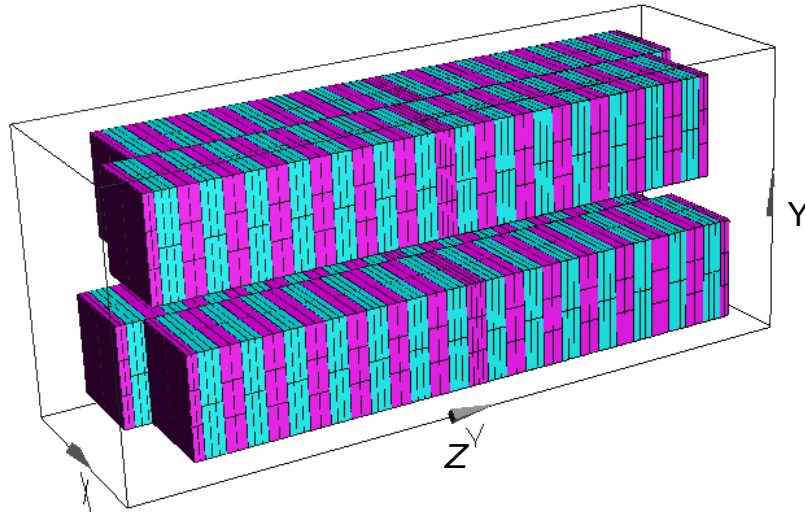


Fig. 1 Short magnet model of the APPLE II undulator with period length $\lambda = 2.6$ cm. Each magnet block has the dimensions 3.0 (X = width) x 3.0 (Y = height) x 0.65 ($\lambda/4$; Z = longitudinal) cm³. The two magnet arrays above and below the mid plane are fixed longitudinally. The phase shift is set to 0.85 cm. The purple magnets generate the vertical magnetic field and the blue magnets the horizontal magnetic field.

The results of the calculations are given in Table 1. This undulator generates both low total power and low power density. Data for those are also included in the table although they would not cause any high heat load issues for the beamline components. The total power and power density scale linearly with the length of the undulator, so it is straightforward to estimate the values for any other length of the undulator.

Table 1: RADIA-calculated effective magnetic fields and first-harmonic energies versus undulator gap for the APPLE II helical undulator with 2.6-cm period length for 7.0-GeV beam energy. For the power calculations, a device length of 2.4 m was assumed and a beam current of 100 mA was used. A magnetic design with NdFeB magnets ($B_r = 1.22$ Tesla) was used.

Undulator Gap (mm)	B_x (Tesla)	B_y (Tesla)	K_x	K_y	E_I (keV) ^a	$P_{density}$ ^b (kW/mrad ²)	P_{total} ^b (kW)
11.0	0.2826	0.2790	0.6863	0.6775	12.22	66.7	1.17
11.5	0.2616	0.2629	0.6352	0.6384	12.74	65.9	1.02
12.0	0.2422	0.2477	0.5882	0.6016	13.22	64.3	0.89
12.5	0.2244	0.2334	0.5450	0.5668	13.68	62.1	0.78
13.5	0.1930	0.2072	0.4686	0.5032	14.48	56.4	0.59
15.0	0.1544	0.1733	0.3749	0.4208	15.45	46.1	0.40

^a Zero-emittance calculation for on-axis radiation for a beam energy of 7.0 GeV.

^b Zero-emittance calculated values at a beam energy of 7.0 GeV and a beam current of 100 mA using B_x and B_y and the full number of undulator periods ($N = 92$), corresponding to a device length L of 2.4 m. Compare versus Undulator A (3.30-cm period): on-axis power density 168 kW/mrad² and total power 6.0 kW at 10.5-mm gap. The power and power density scales linearly with device length L . The total power scales quadratically with the magnetic field.

The gap dependence of the effective K value for both x and y is shown in Fig. 2. The data were taken from Table 1. The gap dependence of the two magnetic fields differs by a small amount due to the fixed phase shift between the jaws; however, it has a negligible effect on the degree of circular polarization and the content of the higher harmonics (see radiation calculations below).

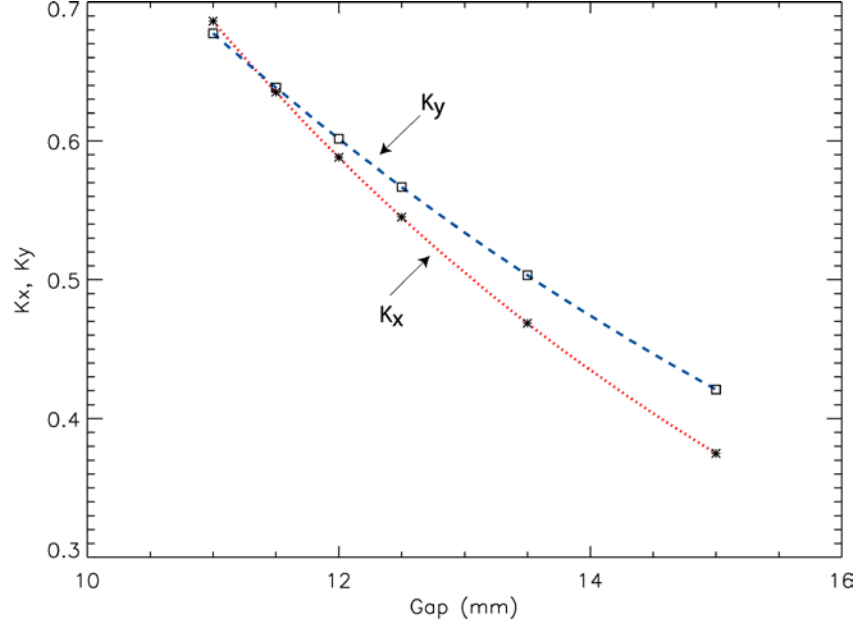


Fig. 2. Calculated gap dependence of the effective K value in the horizontal plane (K_x ; red dotted curve) and in the vertical plane (K_y ; blue dashed curve) for the APPLE II undulator with 2.6-cm period length. The symbols indicated the calculated values and the curves show the interpolated values. The magnetic field in the horizontal plane drops at a higher rate than in the vertical plane when the gap is opened.

The gap dependence of the first-harmonic energy E_1 , is shown in Fig. 3. The first-harmonic energy ranges from 12.2 keV at 11.0-mm gap to 15.5 keV at 15.0-mm gap.

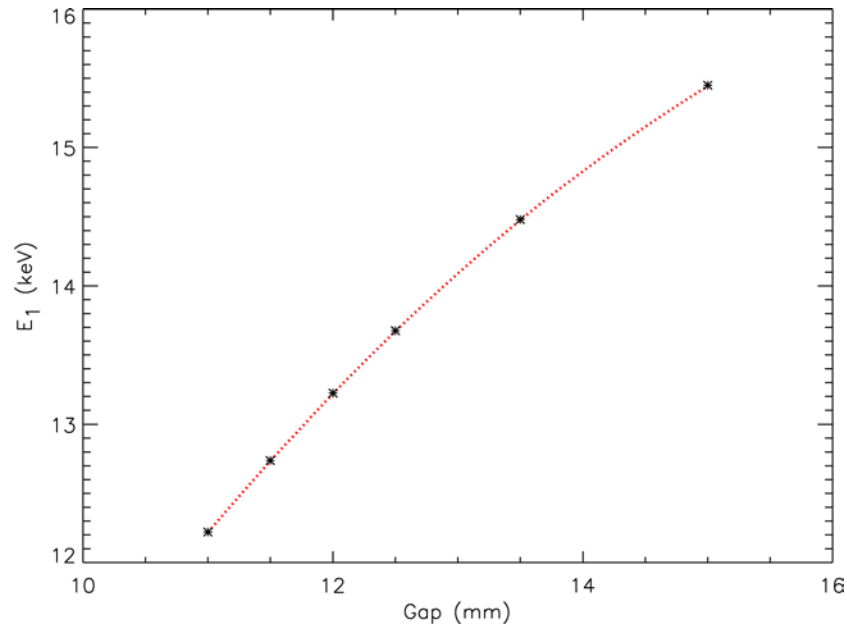


Fig. 3. Gap dependence of the zero-emittance calculated first harmonic energy for the APPLE II undulator with 2.6-cm period length for 7.0-GeV beam energy. The symbols show the calculated values and the curve shows the interpolated values. The minimum energy is 12.2 keV at 11.0-mm gap.

Radiation Calculations

We have performed calculations of the on-axis flux using the APS beam parameters for the 2.5 nm-rad low-emittance lattice for top-up operations. The results of those calculations are presented in this section for the following beam parameters: $E_R = 7.0$ GeV, $I_R = 100$ mA, $\sigma_x = 0.275$ mm, $\sigma_y = 0.009$ mm, $\sigma_{x'} = 0.0113$ mrad, $\sigma_{y'} = 0.0030$ mrad, and beam energy spread 9.6×10^{-4} .

Generally, the shorter the period length, the higher the aperture flux for any given harmonic energy. But, the shorter the period length, the larger the power and power density for any given harmonic energy. The fraction of the emitted power contained in the central cone to the total power drops rapidly with increasing K value, as it is proportional to $1/(1+K_x^2/2+K_y^2/2)^2$ for large K values. Therefore, it is important to keep the K values small. Because the desired K value would be less than 1.0, there are no high heat load issues for this device and the undulator period was determined strictly from the minimum required harmonic energy at minimum gap (11.0 mm). For all calculations, ideal magnetic fields were assumed. For real devices however, the intensities will be reduced slightly for the higher harmonics (not discussed in this note). All devices were assumed to be 2.4 m in length.

On-Axis Flux and Power in the First Harmonic: Helical Undulator versus Undulator A

We compare the aperture flux for the proposed 2.6-cm-period helical undulator with Undulator A in Fig. 4 for the energy range 12 – 15 keV. The chosen rectangular aperture 2.5 (h) x 1.0 (v) mm, located 30 m from the source, covers roughly the central cone of radiation of the first-harmonic energy and may be compared to earlier calculations found elsewhere for other insertion devices.

For a very wide energy bandwidth, which will be used for this beamline, a wider slit such as 5.0 (h) x 5.0 (v) mm may be desirable to capture more flux. This case is shown in Fig. 5. (For the example given here, the aperture approaches the size of the power density profile, and it is substantially larger than the size of the central cone of the first harmonic calculated for a limited bandwidth acceptance.) The calculation of the optimum aperture size will be performed at a later time.

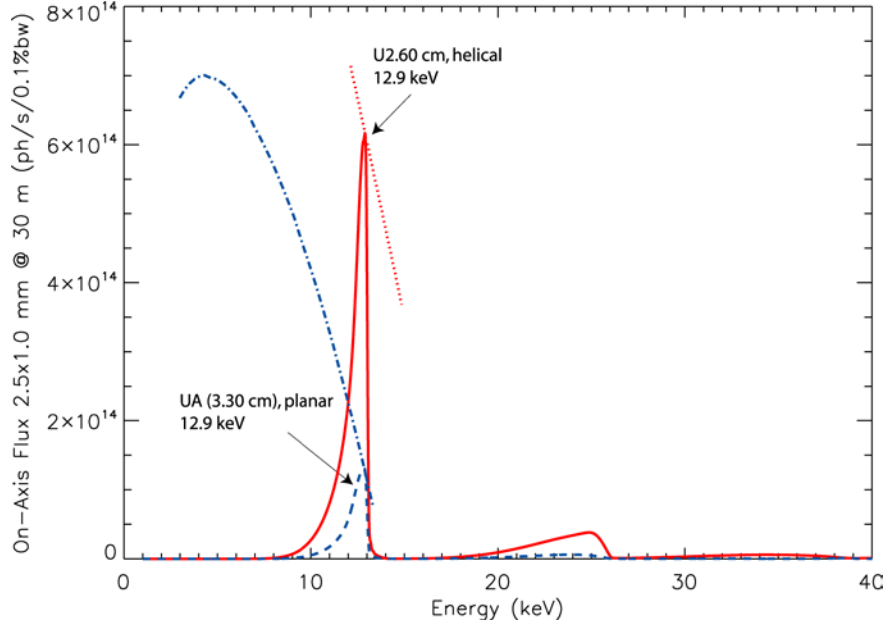


Fig. 4. On-axis flux through a 2.5 (h) \times 1.0 (v) mm rectangular aperture at 30 m for the APPLE II undulator with 2.6-cm period length (red solid curve) compared to Undulator A (3.3-cm period length) (dashed blue curve) for 7.0-GeV beam energy and 100-mA beam current. The undulators were set to generate the first harmonic energy at 12.9 keV (gaps are 11.8 mm for the APPLE II and 30.0 mm for Undulator A). The tuning curves for the first harmonic are shown for the helical undulator (red dotted curve) and Undulator A (blue dotted-dashed curve).

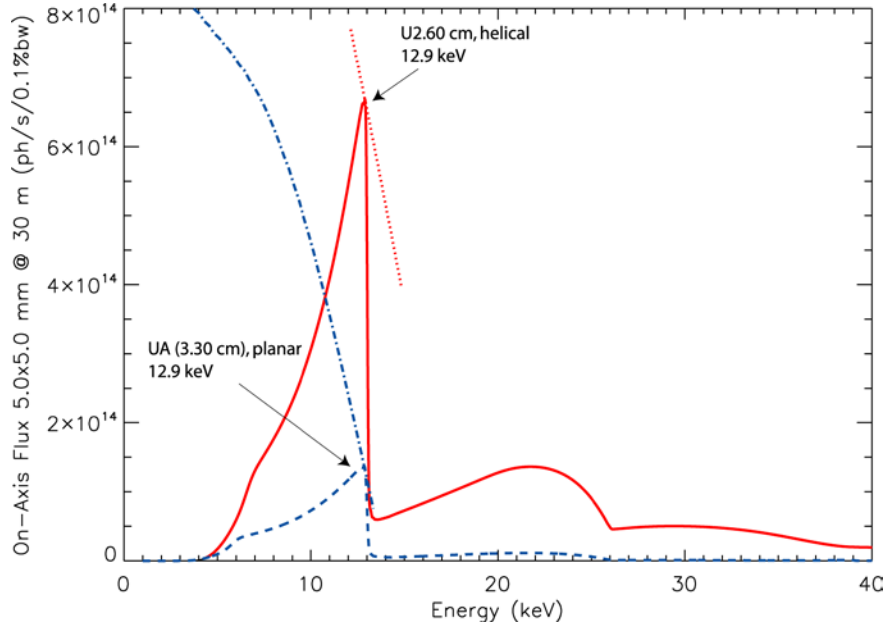


Fig. 5. On-axis flux through a 5.0 (h) \times 5.0 (v) mm rectangular aperture at 30 m for the APPLE II undulator with 2.6-cm period length (red solid curve) compared to Undulator A (3.3-cm period length) (dashed blue curve) for 7.0-GeV beam energy and 100-mA beam current. Other notations are the same as in Fig. 4.

The proposed APPLE II helical undulator outperforms Undulator A by a large margin over the entire energy range. For example, for the small aperture, it produces 4.4 times more power in the central cone of the first harmonic than Undulator A at 12.9 keV, while at the same time generating similar higher harmonic content (the second harmonic for the helical undulator is slightly stronger due to the larger K value). For the very large aperture, the enhancement is almost as large, but the fraction of higher harmonic radiation increases (see Fig. 5). We also note that the flux of the first harmonic radiation of Undulator A drops rapidly above 12 keV and that the full requested energy range up to 15 keV cannot be reached.

The powers and K values of the two undulators are compared in Table 2. For comparison, we have also added information for a planar undulator with the same period length as the helical undulator.

Table 2: Powers and K values of the proposed 2.6-cm-period APPLE II undulator, Undulator A, and a planar 2.6-cm-period undulator. The undulators are 2.4 m long. The beam energy is 7.0 GeV and the beam current is 100 mA.

Undulator Type	K_x	K_y	E (keV) ^a	P_{ApI} (W) ^c	P_{Ap} (W) ^f	R (%) ^g	P_{total} (W)
APPLE II (2.6 cm)	0.612	0.612	12.9	108.8	145.1	75	922
	0.612	0.612	12.9	366.4 ^d	692.0 ^d	53	922
	0.500	0.500	14.2	94.5	117.1	81	615
U2.6 cm (planar)	0.0	0.865	12.9	84.1	174.6	48	922
	0.0	0.707	14.2	75.9	127.7	59	615
Undulator A (3.3 cm)	0.0	0.410	12.9	24.7	30.0	82	127
	0.0	0.410	12.9	87.2 ^d	105.5 ^d	83	127
	0.0	2.13	12.9 ^b	61.7 ^e (20.1)	316.7	19 ^e (6.3)	3422

^a Zero-emittance calculation of the first-harmonic energy for on-axis radiation for a beam energy of 7.0 GeV, except for last entry, which is for the third harmonic.

^b Third-harmonic energy.

^c Aperture power integrated over the first-harmonic energy (< 14.0 keV for $E_l = 12.9$ keV, and < 16.0 keV for $E_l = 14.2$ keV). The aperture size is 2.5 (h) \times 1.0 (v) at 30 m, unless otherwise noted.

^d The aperture size is 5.0 (h) \times 5.0 (v) at 30 m.

^e The energy-integrated aperture power includes the first- and second-harmonic energies. The values in the parentheses relate to the power in the third harmonic only, integrated over 10.0 – 14.0 keV.

^f Aperture power integrated over all energies.

^g Ratio of P_{ApI}/P_{Ap} .

We note that the ratio of the first-harmonic power to the total-aperture power is considerably higher for the helical undulator. For the small aperture at 12.9 keV, the ratio is 27 percentage points higher, and at 14.2 keV it is 22 percentage points higher than for the planar undulator with the same period length. The ratios increase with decreasing K value, and for very small K values they would approach the same value (with very low flux generated). The flux and power of the planar undulator with 2.6-cm period is further discussed in the Appendix.

As was already alluded to, it is not possible to make K_x and K_y the same over the entire gap range (c.f., Fig. 2). Therefore, to study the effect of the difference in actual K value, we examined the performance of the first harmonic at 14.2 keV ($K_x = 0.4830$ and $K_y = 0.5153$). The degree of circular polarization P_3 changed by less than 0.2% near the harmonic energy and the power in the first harmonic dropped by less than 1 W (the ratio dropped less than one percentage point) compared to the ideal case ($K_x = K_y = 0.500$). Both changes are within the accuracy we seek here and may be neglected.

One may envision using the third-harmonic undulator radiation from Undulator A to increase the power in the central cone. However, even though the aperture-limited power increases substantially, most of the power is not contained in the desirable energy band. In other words, the “contamination” at other x-ray energies is large, and the power contained in the central cone of the third harmonic is only about 6% of the total aperture-limited power. Figure 6 compares the helical undulator with Undulator A set to generate the third harmonic at 12.9 keV. The figure clearly shows that only a small fraction of the total power is contained in the third harmonic.

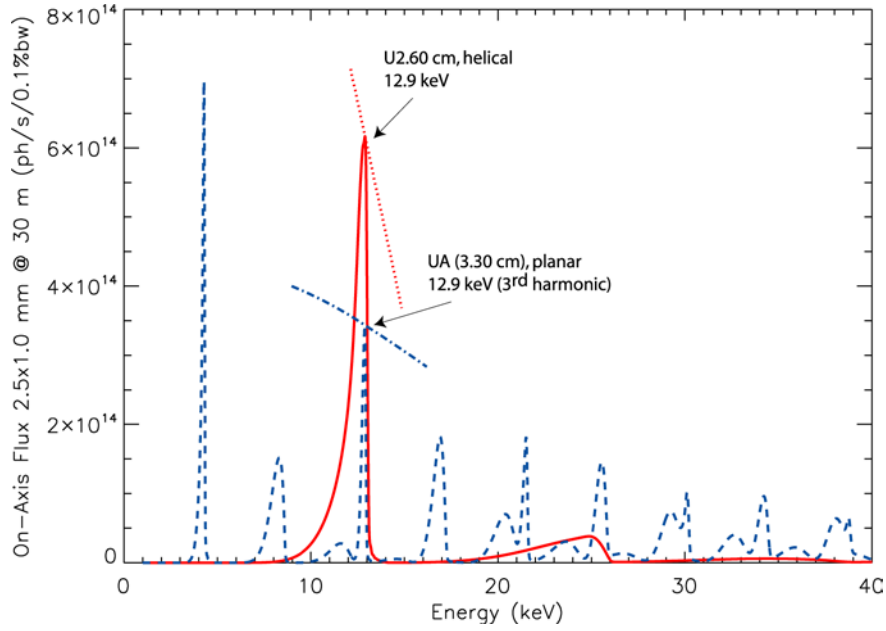


Fig. 6. On-axis flux through a 2.5 (h) \times 1.0 (v) mm rectangular aperture at 30 m for the APPLE II undulator with 2.6-cm period length (red solid curve) and for Undulator A (3.3-cm period length) (dashed blue curve) for 7.0-GeV beam energy and 100-mA beam current. Undulator A was set to generate the *third* harmonic at 12.9 keV (13.0-mm gap). The tuning curve for the first harmonic for the helical undulator (red dotted curve) and for the third harmonic for Undulator A (blue dotted-dashed curve) are shown.

Total Power and Power Density

The total emitted power for the APPLE II undulator ($L = 2.4$ m, $\lambda = 2.6$ cm) is only 1.17 kW at the minimum energy of 12.2 keV. This is much smaller than for Undulator A at closed gap (c.f., Table 1) and would require no further investigations.

The maximum power density for the circular mode is located off-axis in a donut-shaped ring for large K values. However, because the maximum K value is small, the power density still resembles that of a planar undulator. The power densities and spatial flux densities are shown in Figs. 7 – 12 for the cases studied.

For the APPLE II undulator, the power density is much smaller than for Undulator A. As for the total emitted power, this would not cause any high heat load concerns unless a double-length device ($L = 4.8$ m) would be considered. It is apparent from the figures that although the power density may extend over tens of millimeters (at 30 m from the source), the spatial flux density for any given harmonic is much more limited. The small aperture, 2.5 (h) x 1.0 (v) mm at 30 m, matches the size of the central cone and would be a good choice when maximizing the flux while minimizing the bandwidth. However, because a very wide bandwidth may be accepted for this beamline, a large square aperture on the order of 5.0 (h) x 5.0 (v) mm may be a better choice. See Fig. 11, which shows that the power density profile is quite symmetric in x and y for the helical undulator.

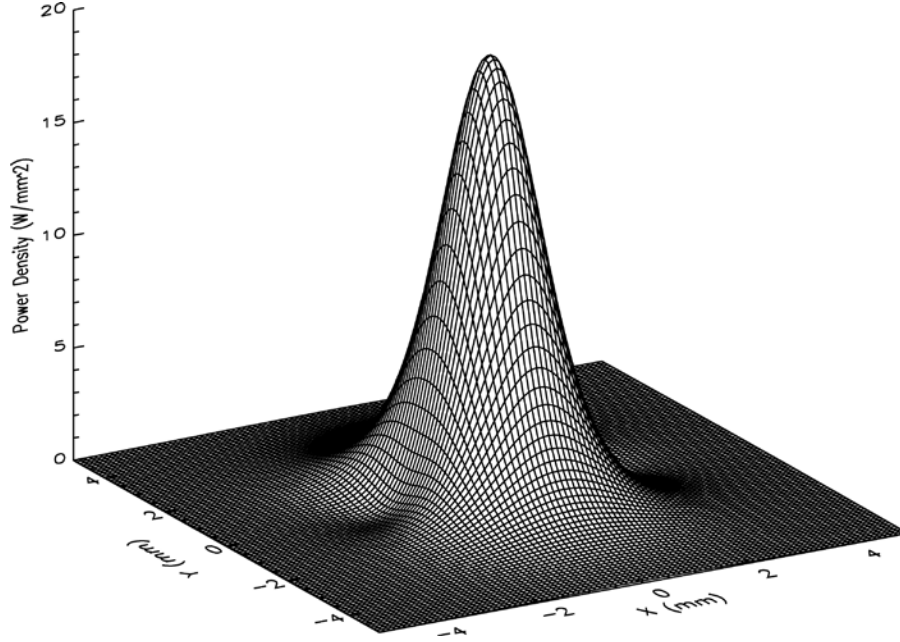


Fig. 7. Power density at 30 m for Undulator A (3.3-cm period length) $K_y = 0.410$ for 7.0-GeV beam energy and 100-mA beam current. The undulator was set to generate the first-harmonic energy at 12.9 keV.

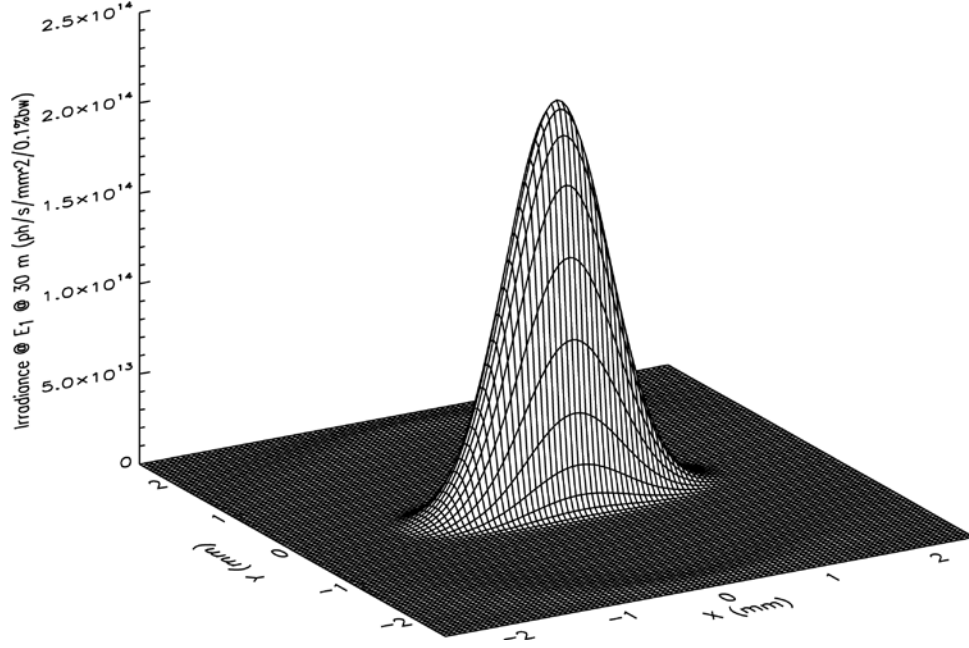


Fig. 8. Spatial photon density at 30 m for Undulator A (3.3-cm period length) at the first-harmonic energy of 12.9 keV ($K_y = 0.410$) for 7.0-GeV beam energy and 100-mA beam current.

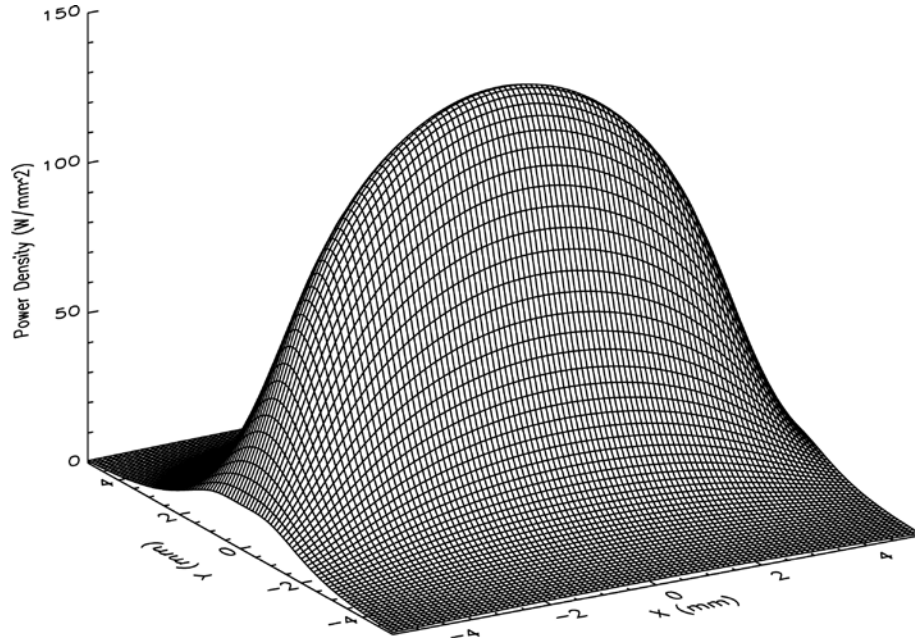


Fig. 9. Power density at 30 m for Undulator A (3.3-cm period length) $K_y = 2.13$ for 7.0-GeV beam energy and 100-mA beam current. The undulator was set to generate the *third*-harmonic energy at 12.9 keV. Large power is being generated and the extent in the horizontal plane is substantial for this case.

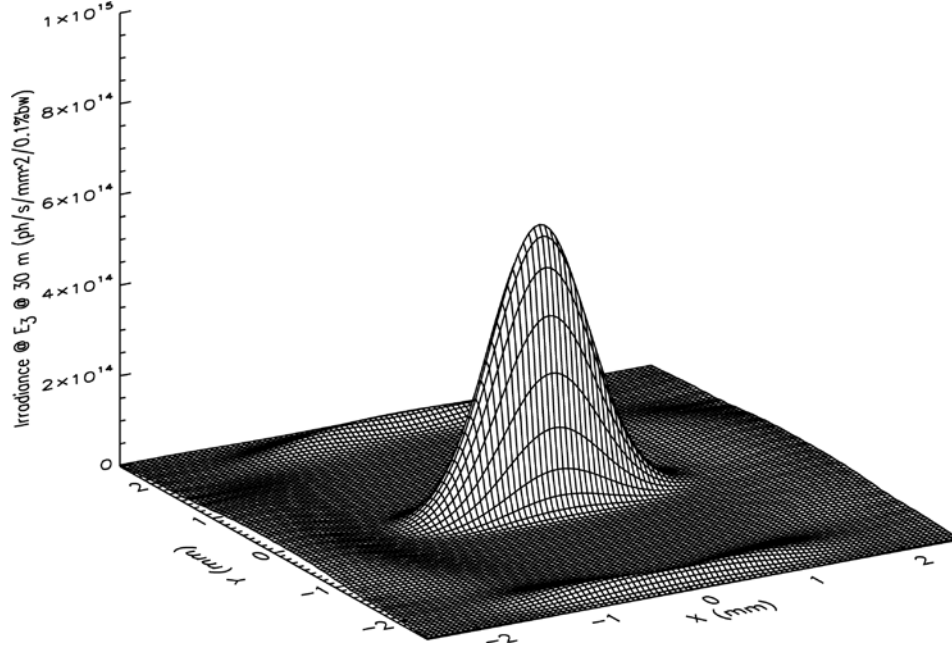


Fig. 10. Spatial photon density at 30 m for Undulator A (3.3-cm period length) at the *third*-harmonic energy of 12.9 keV ($K_y = 2.13$) for 7.0-GeV beam energy and 100-mA beam current.

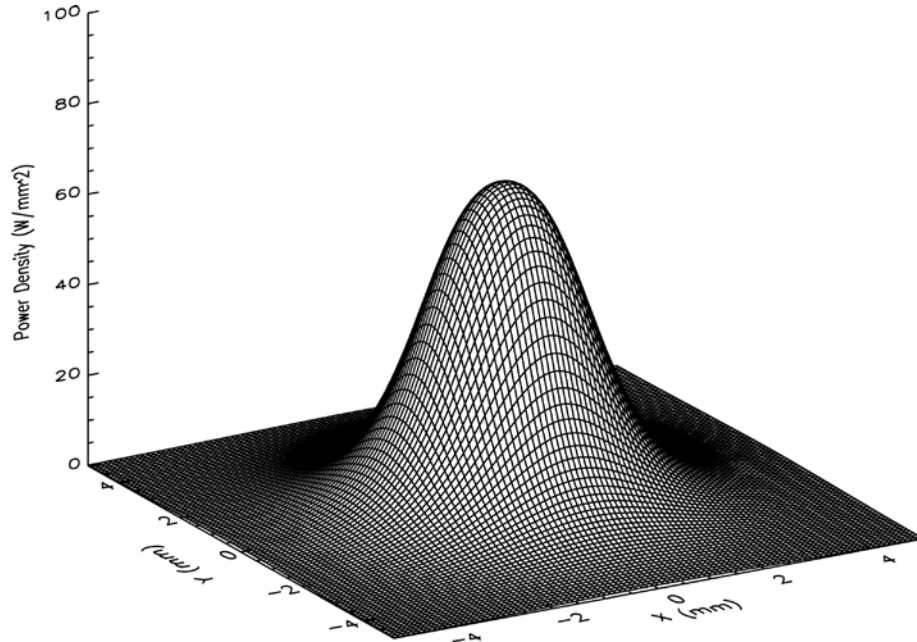


Fig. 11. Power density at 30 m for the APPLE II helical undulator with 2.6-cm period length for $K_x = K_y = 0.612$ for 7.0-GeV beam energy and 100-mA beam current. The undulator was set to generate the first-harmonic energy at 12.9 keV. The power density profile is nearly symmetric in x and y .

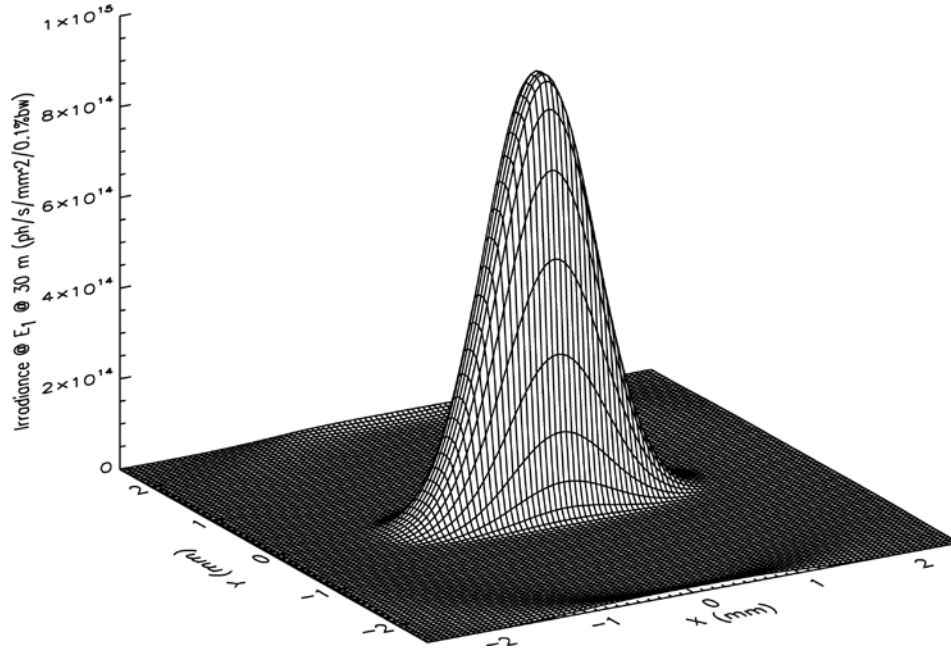


Fig. 12. Spatial photon density at 30 m for the APPLE II helical undulator with 2.6-cm period length at the first-harmonic energy of 12.9 keV ($K_x = K_y = 0.612$) for 7.0-GeV beam energy and 100-mA beam current.

Summary

- The desired first-harmonic energy range from 12 keV to 15 keV can be met with an APPLE II undulator with a period length of 2.6 cm operating at a minimum gap of 11.0 mm.
- Undulator A cannot be used above 13 keV in the first harmonic, and it cannot be used in the third harmonic because too much unwanted radiation is generated.
- The proposed APPLE II undulator would produce over four times more power in the central cone of the first harmonic than Undulator A at 12.9 keV, while maintaining a similar higher-energy x-ray content.
- An undulator generating circularly polarized x-rays is proposed because such a device would show very small “contamination” of high-energy x-rays.
- The undulator would operate with fixed circular polarization because there are no requirements to change the polarization, and it would be designed to fit into the existing vacuum chamber. This in turn simplifies the design and hence reduces the cost.
- The maximum on-axis power density and the maximum total power will not cause any concerns, even for a double-length ($L = 4.8$ m) device using today’s storage ring beam current. For future higher beam current at 200 mA, only a double-length device

may warrant further investigation as the on-axis power density may exceed the limit of the first-generation front-end designs.

- The size of the beamline aperture needs be tailored to the experimental setup for optimum performance. It may be increased from the typical size of 2.5 (h) x 1.0 (v) mm at 30 m to increase the flux because of the large bandwidth acceptance of this beamline. A large aperture will still produce over four times more power in the first harmonic compared to Undulator A.
- If installed in the APS storage ring, this would be the first device of this kind here, although such devices are used at many other facilities (most popular in Europe). Its impact on the APS storage ring operation needs to be investigated before any commitment of such a device can be made.
- A detailed design needs to address an APS specific installation, e.g., attractive and repulsive forces exist between the jaws, although this should not be of major concern because of the short period length.

Appendix

On-Axis Flux and Power in the First Harmonic: Helical Undulator versus Planar Undulator with the Same Period Length

We compare the aperture flux for the proposed 2.6-cm-period helical undulator with a planar undulator with the same period length in Fig. 13. As before, the chosen rectangular aperture $2.5 (h) \times 1.0 (v)$ mm, located 30 m from the source, covers roughly the central cone of radiation of the first harmonic energy. The higher-order harmonics are greatly suppressed for the helical undulator.

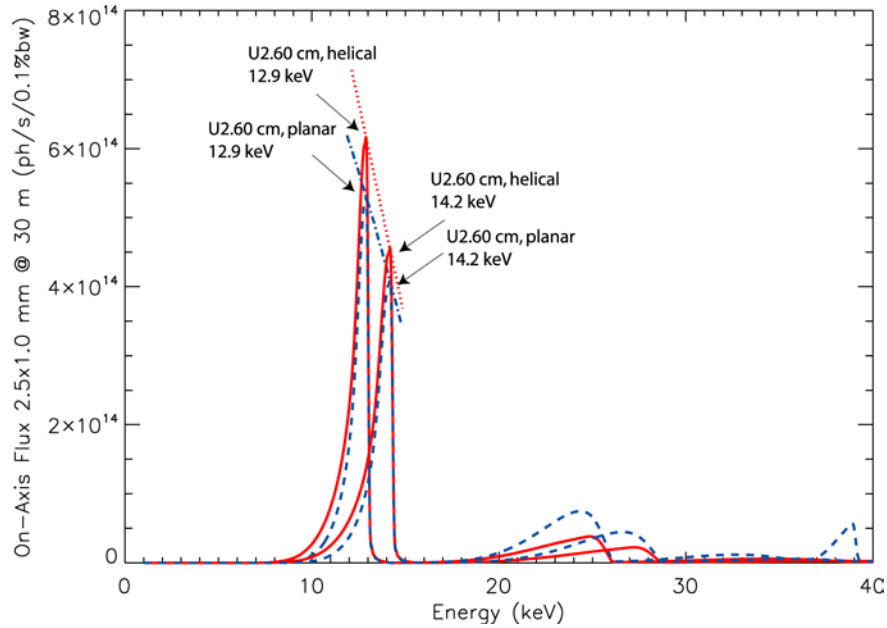


Fig. 13. On-axis flux through a $2.5 (h) \times 1.0 (v)$ mm rectangular aperture at 30 m for the APPLE II undulator with 2.6-cm period length (red solid curves) compared to a planar undulator with the same period length (dashed blue curves) for 7.0-GeV beam energy and 100-mA beam current. The undulators were set to generate the first harmonic energies at 12.9 keV and 14.2 keV (gaps are 11.8 mm and 13.3 mm for the APPLE II, respectively). The tuning curves for the first harmonic are shown for the helical undulator (red dotted curve) and the planar undulator (blue dotted-dashed curve). The first, second, and third harmonics are shown. The higher harmonics are greatly suppressed for the helical undulator.

A summary of the power in the central cone of the first harmonic was given in Table 2. We note that the helical undulator provides both more power and a higher ratio of the first harmonic power to the total power than the planar undulator. The power density and the spatial photon density for the planar undulator are shown in Figs. 14 – 15.

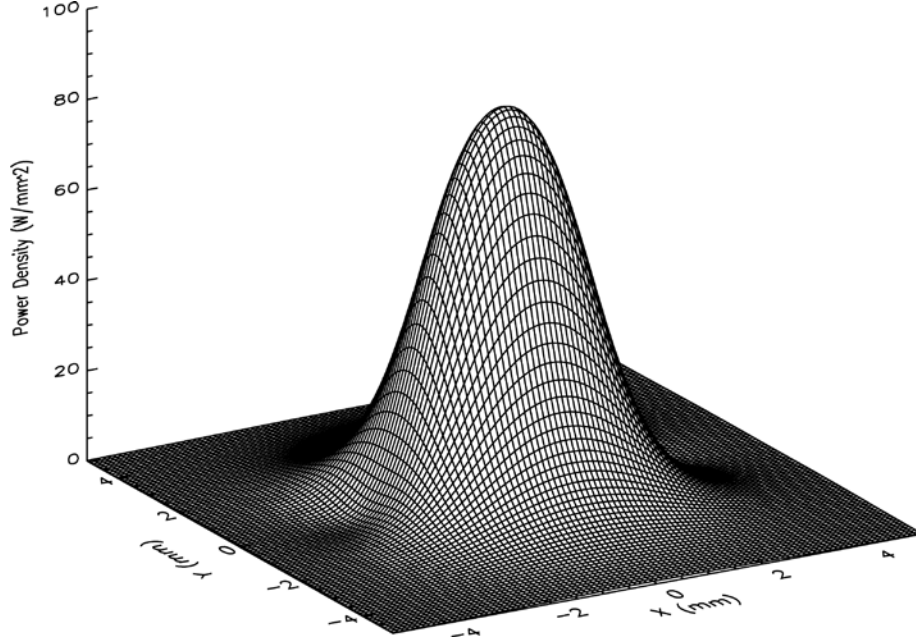


Fig. 14. Power density at 30 m for the planar undulator with 2.6-cm period length for $K_y = 0.865$ for 7.0-GeV beam energy and 100-mA beam current. The undulator was set to generate the first-harmonic energy at 12.9 keV.

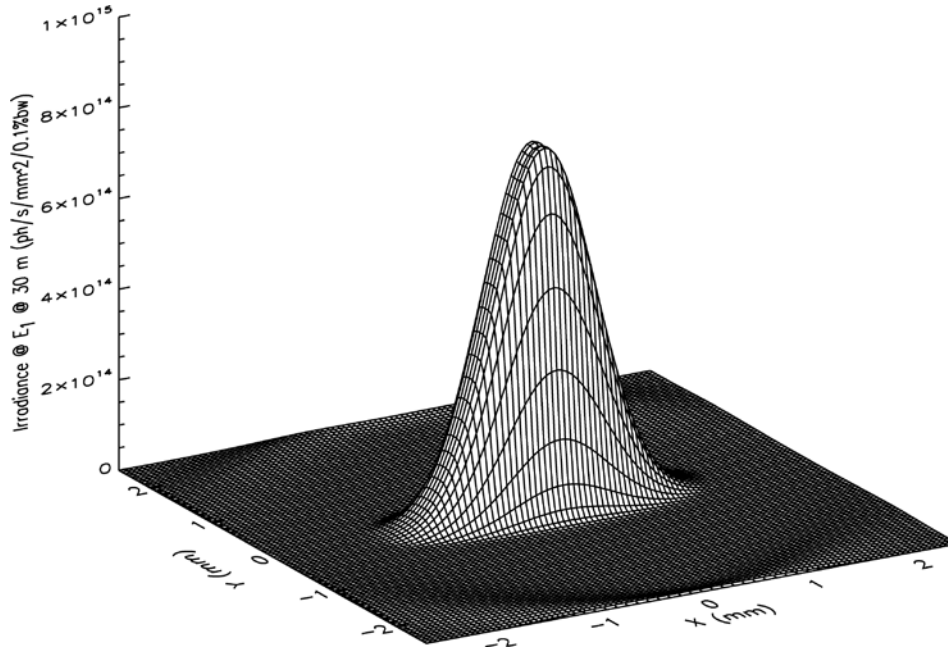


Fig. 15. Spatial photon density at 30 m for the planar undulator with 2.6-cm period length at the first-harmonic energy of 12.9 keV ($K_y = 0.865$) for 7.0-GeV beam energy and 100-mA beam current.

References

¹ Manuel Sánchez del Río and Roger J. Dejus, “XOP 2.1 - A New Version of the X-ray Optics Software Toolkit,” Proceedings of the 8th International Conference on Synchrotron Radiation Instrumentation, August 25-29, 2003, San Francisco, CA, AIP Conf. Proc. 705, 784-787 (2004).

² R. Dejus, private communication.

³ Code RADIA. Web site: <http://www.esrf.fr/Accelerators/Groups/InsertionDevices/Software>

⁴ Shigemi Sasaki, “Analyses for a planar variably-polarizing undulator,” Nucl. Instrum. Methods A 347 (1994) 83-86.